Available online at www.pelagiaresearchlibrary.com

Pelagia Research Library

Advances in Applied Science Research, 2013, 4(6):285-306

ISSN: 0976-8610
CODEN (USA): AASRFC

Closed form solution of heat and mass transfer past an inclined oscillating surface with Newtonian heating under the effect of thermal radiation and mass diffusion

Preeti Jain and R. C. Chaudhary

Department of Mathematics, University of Rajasthan, Jaipur, India

---

ABSTRACT

An exact solution of the unsteady free convection boundary-layer flow of an incompressible fluid past an inclined oscillating plate with the flow generated by Newtonian heating in the presence of radiation is presented here. The resulting coupled linear partial differential equations for the velocity, the temperature and the concentration are non-dimensionalized and their solutions have been obtained in closed form with the help of Laplace-transform technique. The obtained solutions satisfy governing equations as well as the boundary conditions. A parametric study of all involved parameters is conducted and a representative set of numerical results for the velocity, temperature, concentration, skin-friction, Nusselt number and Sherwood number is illustrated graphically and physical aspects of the problem are discussed in detail.

Keywords: Newtonian heating, oscillating plate, Unsteady free convection, Heat transfer, Mass transfer, thermal Radiation, inclined plate, Incompressible fluid.

INTRODUCTION

The phenomena of free convection arise in the fluid when temperature change causes density variation leading to buoyancy forces acting on the fluid elements. Natural convection heat transfer plays an important role in our environment and in many engineering devices. This can be seen in our everyday life in the atmospheric flow, which is driven by temperature differences. Soundalgekar [1] first presented an exact solution to the flow of a viscous incompressible fluid past an impulsively started infinite vertical plate by Laplace transform technique. In this case the plate was assumed to be isothermal. Free convection effects on flow past an exponentially accelerated vertical plate was studied by Singh and Naveen Kumar [2]. The skin friction for accelerated vertical plate has been studied analytically by Hossain and Shayo [3].Das et al. [4] discussed transient free convection flow past an infinite vertical plate with periodic temperature variation and Soundalgekar et al. [5] studied the same problem with periodic heat flux. An excellent review of existing theoretical and experimental work on unsteady boundary layers can be found in books by Stuart [6], Telionis [7] and Pop [8]. Raptis et al. [9] studied the free convection flow of water near a moving plate. Das et al.[10] analyzed the flow problem with periodic temperature variation and Muthucumaraswamy [11] considered the natural convection with variable surface heat flux. Chandran [12] presented natural convection with ramped wall temperature.

Furthermore, there are applications of interest in which combined heat and mass transfer by natural convection occurs between a moving material and the ambient medium, such as the design and operation of chemical

processing equipment, design of heat exchangers, transpiration cooling of a surface, chemical vapor deposition of solid layers, flow in a desert cooler, nuclear reactors, and many manufacturing processes like hot rolling, hot extrusion, wire drawing, continuous casting, and fiber drawing. In view of such application, Gebhart and Pera [13] studied the effects of mass transfer on a steady free convection flow past a semi infinite vertical plate by the similarity method, and it was assumed that the concentration level of the diffusing species in the fluid medium was very low. This assumption enabled them to neglect the diffusion-thermo and the thermo-diffusion effects, as well as the interfacial velocity at the wall due to species diffusion. Following this assumption, Soundalgekar [14] studied the effects of mass transfer on the free convection flow past an impulsively started infinite vertical plate and presented an exact solution by the Laplace transform method. Soundalgekar and his co-researchers [15-18] investigated the effects of simultaneous heat and mass transfer on free convection flow past an infinite vertical plate under different physical situations. An analytical study to examine the mass transfer effects flow past an exponentially accelerated vertical plate was performed by Jha et al.[19] and Muthucumaraswamy et al.[20, 21]. Recently, Narahri[22] used Laplace transform technique to study the mass transfer and free convection current effects on unsteady viscous flow with ramped wall temperature. Saravana etal. [23] studied the mass transfer effects on MHD viscous flow past an impulsively started infinite vertical plate with constant mass flux.

In all the studies mentioned above the plate was either (i) moving with uniform velocity or (ii) it was uniformly accelerated or (iii) there was exponentially accelerated motion of the plate. However flow past a vertical plate oscillating in its own plane has many industrial applications. Free convection flow along a harmonically oscillating plate has many industrial applications. The first exact solution of the Navier-Stokes equation was given by Stokes [24], which is concerned with the flow of incompressible fluid past a horizontal plate oscillating in its own plane. Such a flow past an infinite vertical plate oscillating in its own plane was first studied by Soundalgekar [25]. Similar problem of flow past an oscillating plate was investigated by Turbatu et al. [26], Revankar [27] and Gupta et al. [28]. Gupta employed the Laplace transform technique to study the flow in the Ekman layer on an oscillating plate. Further, mass transfer effects on flow past an oscillating plate considered by Lahurikar et al. [29].

In all these investigations the effects of radiation is not taken into account. When the temperature of the surrounding fluid is rather high, radiation effects on the flow become significant. In some industrial applications such as glass production, furnace design, thermonuclear fusion, casting and levitation and in space technology applications such as cosmic flight aerodynamics, rocket propulsion systems, plasma physics, and space craft reentry aerothermodynamics which operate at higher temperature, radiation effects play an important role. Keeping in view this fact, Hossain et al. [29] determined the effect of radiation on the natural convection flow of an optically thick, viscous, incompressible flow past a heated vertical porous plate with a uniform surface temperature and a uniform rate of suction, where the radiation was included by assuming the Rosseland diffusion approximation. Raptis and Perdikis [30] studied the effects of thermal radiation and free convective flow past a uniformly accelerated vertical plate. Soundalgekar et al. [31] further presented exact solution to radiation effect on flow past an impulsively started vertical plate. Radiation effects on mixed convection along an isothermal vertical plate were studied by Hossain and Takhar [32]. Makinde [33] focused on the thermal radiation and mass transfer past a moving porous plate. Muthucumaraswamy [34, 35] obtained exact solutions taking into account the effects of thermal radiation under different boundary conditions. Recently, Deka and Das [36] investigated radiation effects past a vertical plate using ramped wall temperature, Jana and Ghosh [37] investigated radiative heat transfer in the presence of indirect natural convection. Effects of radiation on unsteady MHD free convective flow past an oscillating vertical porous plate embedded in a porous medium with oscillatory heat flux was studied by Manna etal.[39]. Diffusion-thermo and radiation effects on mhd free convective heat and mass transfer flow past an infinite vertical plate in the presence of a chemical reaction of first order was discussed by Raveendra Babu [40] and his co-researchers. Further, Seshaiah [41] etal. analyzed thermal diffusion and radiation effects on unsteady MHD free convection heat and mass transfer flow past a linearly accelerated vertical plate with variable temperature and mass diffusion.

The above studies did not access the flow from an inclined surface, a regime of considerable importance in glass manufacturing, external aerosol particle deposition processes (Jayaraj[42]), powder technology fluidization processes (Doroodchi et al.[43]), film cooling chemical engineering systems electronic circuit cooling mechanisms, solar energy collector (Beg[44]).Recently, thermal radiation effects on unsteady hydromagnetic gas flow along an inclined plane with indirect natural convection has been investigated by Ghosh et al.[45]. Barik [46] discussed the mass transfer and radiation effect on an exponentially accelerated inclined porous plate with variable temperature in the presence of heat source. Similar problem was studied by Reddy [47].

In all the studies cited above the flow is driven either by a prescribed surface temperature or by a prescribed surface heat flux. Here a different driving mechanism for unsteady free convection along a vertical surface is considered; here the flow is set up by Newtonian heating from the surface. Heat transfer characteristic are dependent on the thermal boundary conditions. In general there are four common heating processes specifying the wall-to-ambient temperature distributions, prescribed surface heat flux distributions, conjugate conditions where heat is specified through a bounding surface of finite thickness and finite heat capacity. The interface temperature is not known a priori but depends on the intrinsic properties of the system, namely the thermal conductivity of the fluid and solid respectively. Newtonian heating, where the heat transfer rate from the bounding surface with a finite heat capacity is proportional to the local surface temperature and is usually termed conjugate convective flow. This configuration occurs in many important engineering devices, for example:

(i) In heat exchangers where the conduction in solid tube wall is greatly influenced by the convection in the fluid flowing over it.
(ii) For conjugate heat transfer around fins where the conduction within the fin and the convection in the fluid surrounding it must be simultaneously analyzed in order to obtain the vital design information.
(iii) In convective flows set up when the bounding surfaces absorbs heat by solar radiation.

Therefore we conclude that the conventional assumption of no interaction of conduction-convection coupled effects is not always realistic and it must be considered when evaluating the conjugate heat transfer processes in many practical engineering applications. The Newtonian heating condition has been only recently used in convective heat transfer. Merkin [48] was the first to consider the free-convection boundary-layer over a vertical flat plate immersed in a viscous fluid whilst [49, 50, 51] considered the cases of vertical and horizontal surfaces embedded in a porous medium. The studies mentioned in [49 - 51] deal with steady free convection. In this area the authors of this [52, 53] were the first one to give exact solution to the unsteady free convection boundary-layer flow from a flat vertical plate with Newtonian heating and the solution was obtained in closed form using Laplace transform technique. Our work was further extended by Narahari and Nayan [54], Raju et al. [55] and Narahari and Ishak [56] in which they incorporated the effects of thermal radiation and mass transfer with Newtonian heating under different boundary conditions like impulsively started plate, exponentially accelerated plate, moving plate etc. An exact solution of the unsteady free convection flow of a viscous incompressible, optically thin, radiating fluid past an impulsively started vertical porous plate with Newtonian heating was investigated by Mebine and Adigio[57].

To the best of authors' knowledge, so far, no study has been reported in the literature which investigates the unsteady free convection flow of an incompressible viscous fluid past an inclined plate with Newtonian heating and constant mass diffusion. The plate is oscillating in its own plane. In this study, the equations of the problem are first formulated and transformed into their dimensionless forms where the Laplace transform method is applied to find the exact solutions for velocity, temperature and concentration. Moreover, expressions for skin friction, Nusselt number, and Sherwood number are obtained and are plotted graphically and discussed for the pertinent flow parameters.

Mathematical Analysis

Consider the unsteady free convective flow of a viscous incompressible, absorbing-emitting, non-scattering, optically-thick fluid past an tilted plate inclined at an angle α to the vertical. The plate is oscillating in its own plane. The x^*-axis is taken along the oscillating plate and y^*-axis is chosen normal to the plate. Initially, for time $t^* \leq 0$, the plate and fluid are at the constant temperature T_∞^* and concentration C_∞^* to C_∞^* in a stationary condition. At time $t^* \geq 0$, the plate starts an oscillatory motion in its plane with the velocity with $U_0 \cos(\omega^* t^*)$, where U_0 is the amplitude and ω^* is the frequency of the plate oscillations. It is assumed that rate of heat transfer from the surface is proportional to the local surface temperature T^* and the concentration level near the plate is raised from C_∞^* to C_w^*. Since the plate is considered infinite in the x^* direction, hence all physical variables will be independent of x^*. Therefore, the physical variables are functions of y^* and t^* only. Applying the Boussinesq approximation which states that all fluid properties are constant with the exception of the density variation in the buoyancy term, the free convective is governed by the following equations:-

$$\frac{\partial u^*}{\partial t^*} = \nu \frac{\partial^2 u^*}{\partial y^{*2}} + g\beta(T^* - T_\infty^*)\cos\alpha + g\beta^*(C^* - C_\infty^*)\cos\alpha \quad (1)$$

$$\rho C_p \frac{\partial T^*}{\partial t^*} = k\frac{\partial^2 T^*}{\partial y^{*2}} - \frac{\partial q_r}{\partial y^*} \tag{2}$$

$$\frac{\partial C^*}{\partial t^*} = D \frac{\partial^2 C^*}{\partial y^{*2}} \tag{3}$$

With the following initial and boundary conditions:

$$\left.\begin{aligned} & t^* \le 0 : u^* = 0, \quad T^* = T_\infty^*, \quad C^* = C_\infty^* \qquad \text{for all } y^* > 0 \\ & t^* > 0 : u^* = U_0 \cos\omega^* t^*, \quad \frac{\partial T^*}{\partial y^*} = -\frac{h}{k} T^*, C^* = C_w^* \text{ at } y^* = 0 \\ & \qquad : u^* = 0, \qquad T^* \to T_\infty^*, C^* \to C_\infty^* \qquad \text{as } y^* \to \infty \end{aligned}\right\} \tag{4}$$

The radiation heat flux under Rosseland approximation [58] is expressed by

$$q_r = -\frac{4\sigma}{3k^*}\frac{\partial^4 T^*}{\partial y^*} \tag{5}$$

This model is valid for optically-thick media in which thermal radiation propagates only a limited distance prior to experiencing scattering or absorption. The local thermal radiation intensity is due to radiation emanating from proximate locations in the vicinity of which emission and scattering are comparable to the location of interest. For zones where conditions are appreciably different thermal radiation has been shown to be greatly attenuated before arriving at the location under consideration. The energy transfer depends on conditions only in the area adjacent to the plate regime i.e. the boundary layer regime. Rosseland's model yields accurate results for intensive absorption i.e. optically-thick flows which are optically far from the bounding surface. It is assumed that the temperature difference within the flow are sufficiently small and then (5) can be linearized by expanding T^{*4} into Taylor series about T_∞^*, which after neglecting higher order terms takes the form:

$$T^{*4} \cong 4T_\infty^{*3}T^* - 3T_\infty^{*4} \tag{6}$$

In view of (5) and (6), (2) reduces to

$$\rho C_p \frac{\partial T^*}{\partial t^*} = \left(k + \frac{16\sigma T_\infty^{*3}}{3k^*}\right)\frac{\partial^2 T^*}{\partial y^{*2}} \tag{7}$$

To reduce the above equations into their non-dimensional forms, we introduce the following non-dimensional quantities:-

$$\left.\begin{aligned} & u = \frac{u^*}{U_0}, t = \frac{t^* U_0^2}{\nu}, y = \frac{y^* U_0}{\nu}, \omega = \frac{\omega^* \nu}{U_0^2} \\ & \theta = \frac{T^* - T_\infty^*}{T_\infty^*}, C = \frac{C^* - C_\infty^*}{C_w^* - C_\infty^*}, \Pr = \frac{\mu C_p}{k}, Sc = \frac{\nu}{D} \\ & Gr = \frac{\nu g \beta T_\infty^*}{U_0^3}, Gm = \frac{\nu g \beta^* (C_w^* - C_\infty^*)}{U_0^3}, R = \frac{16\sigma T_\infty^{*3}}{3k k^*} \end{aligned}\right\} \tag{8}$$

Substituting the transformation (8) into equations (1), (3) and (7), we obtain the following non-dimensional partial differential equations:

$$\frac{\partial u}{\partial t} = \frac{\partial^2 u}{\partial y^2} + Gr\,\theta\cos\alpha + Gm\,C\cos\alpha \tag{9}$$

$$\Pr\frac{\partial \theta}{\partial t} = (1+R)\frac{\partial^2 \theta}{\partial y^2} \tag{10}$$

$$Sc\frac{\partial C}{\partial t} = \frac{\partial^2 C}{\partial y^2} \tag{11}$$

The corresponding initial and boundary conditions in non-dimensional form are:

$$\left.\begin{array}{l} t \le 0 : u = 0,\ \theta = 0,\ C = 0 \quad \text{for all } y > 0 \\ t > 0 : u = \cos\omega t,\ \dfrac{\partial\theta}{\partial y} = -\gamma(1+\theta),\ C = 1 \ \text{at } y = 0 \\ \quad\ : u \to 0,\ \theta \to 0, C \to 0 \quad \text{as } y \to \infty \end{array}\right\} \tag{12}$$

Where,

$\gamma = \dfrac{h\nu}{kU_0}$ is the Newtonian heating parameter, when $\gamma = 0$ then $\theta = 0$ which physically corresponds that no heating from the plate exists [59,60], Gr is the Grashof number, Gm is the modified Grashof number, Pr is the Prandtl number, Sc is the Schimdt number and R is the Radiation parameter respectively. Radiation parameter embodies the relative contribution of heat transfer by thermal radiation to thermal conduction. Large R (>1) values therefore correspond to thermal radiation dominance and small values (<1) to thermal conduction dominance (Siegel and Howell). For R = 1 both conduction and radiative heat transfer modes will contribute equally to the regime. Clearly the term in r. h. s. of (10) is an augmented diffusion term i.e. with R = 0, thermal radiation vanishes and eqn. (10) reduces to the familiar unsteady one-dimensional conduction-convection equation. Rests of the physical variables are defined in Nomenclature.

Analytical solutions by the Laplace transform method

The thermal and concentration equations (10) and (11) are uncoupled from the momentum equation (9). One can therefore solve for the temperature variable θ(y, t) and concentration variable C(y, t) whereupon the solution of u(y, t) can also be obtained, using Laplace transform technique. The Laplace transform method solves differential equations and corresponding initial and boundary value problems. The Laplace transform has the advantage that it solves initial value problems directly without determining first a general solution and non-homogeneous differential equations without solving first the corresponding homogeneous equations. Applying the Laplace transform with respect to time t to the eqs. (9) - (11) we get,

$$\left.\begin{array}{l} q\,\bar{u}(y,q) - u(y,0) = \dfrac{d\,\bar{u}(y,q)}{dy^2} + Gr\cos\alpha\,\bar{\theta}(y,q) + Gm\cos\alpha\,\bar{C}(y,q) \\ \Pr\left[q\,\bar{\theta}(y,q) - \theta(y,0)\right] = (1+R)\dfrac{d^2\bar{\theta}(y,q)}{dy^2} \\ Sc\left[q\,\bar{C}(y,q) - C(y,0)\right] = \dfrac{d^2\bar{C}(y,q)}{dy^2} \end{array}\right\} \tag{13}$$

Here,

$\bar{u}(y,q) = \int_0^\infty e^{-qt}u(y,t)dt,\ \bar{\theta}(y,q) = \int_0^\infty e^{-qt}\theta(y,t)dt$ and $\bar{C}(y,q) = \int_0^\infty e^{-qt}C(y,t)dt$ denotes Laplace transforms of $u(y,t),\ \theta(y,t)$ and $C(y,t)$ respectively.

Using the initial condition (12), we get

$$\left.\begin{aligned}&\frac{d\,\bar{u}(y,q)}{d\,y^2}-q\,\bar{u}(y,q)+Gr\,\cos\alpha\,\bar{\theta}(y,q)+Gm\,\cos\alpha\,\bar{C}(y,q)=0\\&\frac{d^2\,\bar{\theta}(y,q)}{d\,y^2}-q\left(\frac{Pr}{1+R}\right)\bar{\theta}(y,q)=0\\&\frac{d^2\,\bar{C}(y,q)}{d\,y^2}-q\,Sc\,\bar{C}(y,q)=0\end{aligned}\right\} \tag{14}$$

The corresponding transformed boundary conditions are:

$$\left.\begin{aligned}&\bar{u}\,(y,q)=\frac{q}{q^2+\omega^2}\\&\frac{d\bar{\theta}(y,q)}{d\,y}=-\gamma\left[\frac{1}{q}+\bar{\theta}(y,q)\right]\\&\bar{C}(y,q)=\frac{1}{q}\,at\,y=0\\&\bar{u}\,(y,q)\to 0,\bar{\theta}(y,q)\to 0,\bar{C}(y,q)\to 0\quad as\ y\to\infty\end{aligned}\right. \tag{15}$$

The solutions of (14) subject to the boundary conditions (15) are:

$$\begin{aligned}\bar{u}\,(y,q)=&\frac{1}{2(q+iw)}e^{-y\sqrt{q}}+\frac{1}{2(q-iw)}e^{-y\sqrt{q}}+\frac{ac}{q^2(\sqrt{q}-c)}e^{-y\sqrt{q}}\\&-\frac{ac}{q^2(\sqrt{q}-c)}e^{-y\sqrt{q\,Pr_{eff}}}+\frac{b}{q^2}e^{-y\sqrt{q}}-\frac{b}{q^2}e^{-y\sqrt{qSc}}\\\bar{\theta}\,(y,q)=&\frac{c}{q(\sqrt{q}-c)}e^{-y\sqrt{q\,Pr_{eff}}}\\\bar{C}\,(y,q)=&\frac{1}{q^2}e^{-y\sqrt{qSc}}\end{aligned} \tag{16}$$

Where,

$a=\dfrac{Gr\cos\alpha}{Pr_{eff}-1}, b=\dfrac{Gm\cos\alpha}{Sc-1}, c=\dfrac{\gamma}{\sqrt{Pr_{eff}}}$ and $Pr_{eff}=\dfrac{Pr}{1+R}$, Pr_{eff} is the effective Prandtl number

By taking the inverse Laplace transform of (16) the solutions are derived as:

$$\theta(y,t)=F_4(y\sqrt{Pr_{eff}},t,c) \tag{17}$$

$$C(y,t)=F_1(y\sqrt{Sc},t) \tag{18}$$

$$\begin{aligned}u(y,t)=&\frac{1}{2}[F_5(y,t,-i\,\omega)+F_5(y,t,i\,\omega)]-\frac{a}{c^2}\left[F_4(y\sqrt{Pr_{eff}},t,c)-F_4(y,t,c)\right]\\&+\frac{a}{c}\left[F_2(y\sqrt{Pr_{eff}},t)-F_2(y,t)\right]+a\left[F_3(y\sqrt{Pr_{eff}},t)-F_3(y,t)\right]\\&-b\left[F_3(y\sqrt{Sc},t)-F_3(y,t)\right]\end{aligned} \tag{19}$$

Note that the above solution for the velocity variable given by equation (19) is not valid for fluids with Prandtl number and Schimdt number unity (ie. $Pr_{eff} \neq 1$ and $Sc \neq 1$). A Schmidt number of unity (Sc = 1) indicates that momentum and mass transfer by diffusion are comparable, and velocity and concentration boundary layers almost coincide with each other. As the Prandtl number is a measure of the relative importance of the viscosity and thermal conductivity of the fluid, the case Pr = 1 corresponds to those fluids whose momentum and thermal boundary layer thickness are of the same order of magnitude. Moreover the exact solutions of the free convection problem

Case I: When $Pr_{eff} \neq 1$and Sc = 1 is given below:

$$u(y,t)=\frac{1}{2}[F_5(y,t,-i\omega)+F_5(y,t,i\omega)]-\frac{a}{c^2}\left[F_4(y\sqrt{Pr_{eff}},t,c)-F_4(y,t,c)\right]$$
$$+\frac{a}{c}\left[F_2(y\sqrt{Pr_{eff}},t)-F_2(y,t)\right]+a\left[F_3(y\sqrt{Pr_{eff}},t)-F_3(y,t)\right] \quad (20)$$
$$+\frac{y\,Gm\cos\alpha}{2}F_2(y,t)$$

Case II: When $Sc \neq 1$and $Pr_{eff} = 1$ is given below:

$$u(y,t)=\frac{1}{2}[F_5(y,t,-i\omega)+F_5(y,t,i\omega)]-b\left[F_3(y\sqrt{Sc},t)-F_3(y,t)\right]$$
$$+\frac{y\,Gr\cos\alpha}{2\gamma}F_4(y,t,\gamma) \quad (21)$$

Case III: When Sc = 1and Pr_{eff} = 1is given below:

$$u(y,t)=\frac{1}{2}[F_5(y,t,-i\omega)+F_5(y,t,i\omega)]+\frac{y\,Gr\cos\alpha}{2\gamma}\left[F_4(y,t,\gamma)\right]-\frac{y\,Gr\cos\alpha}{2}\left[F_2(y,t)\right]$$
$$+\frac{y\,Gm\cos\alpha}{2}\left[F_2(y,t)\right] \quad (22)$$

Here,

$$F_1(v,t)=\operatorname{erfc}\left(\frac{v}{2\sqrt{t}}\right)$$
$$F_2(v,t)=2\sqrt{\frac{t}{\pi}}\,e^{-v^2/4t}-v\operatorname{erfc}\left(\frac{v}{2\sqrt{t}}\right)$$
$$F_3(v,t)=\left(\frac{v^2}{2}+t\right)\operatorname{erfc}\left(\frac{v}{2\sqrt{t}}\right)-v\sqrt{\frac{t}{\pi}}\,e^{-v^2/4t}$$
$$F_4(v,t,\psi)=e^{(\psi^2 t-\psi v)}\operatorname{erfc}\left(\frac{v}{2\sqrt{t}}-\psi\sqrt{t}\right)-\operatorname{erfc}\left(\frac{v}{2\sqrt{t}}\right)$$
$$F_5(v,t,\psi)=\frac{1}{2}e^{(\psi t)}\left[e^{-v\sqrt{\psi}}\operatorname{erfc}\left(\frac{v}{2\sqrt{t}}-\sqrt{\psi t}\right)+e^{v\sqrt{\psi}}\operatorname{erfc}\left(\frac{v}{2\sqrt{t}}+\sqrt{\psi t}\right)\right] \quad (23)$$

erfc (x) being the complementary error function defined by

$$\operatorname{erfc}(x) = 1-\operatorname{erf}(x),\ \operatorname{erf}(x) = \frac{2}{\sqrt{\pi}}\int_0^x \exp(-\eta^2)\,d\eta$$

$$\operatorname{erfc}(0) = 1,\ \operatorname{erfc}(\infty)=0.$$

and erfc ($x_1 + iy_1$) is the complementary error function of the complex argument which can be calculated in terms of tabulated numerical values of the auxiliary function $W_1(z)$, $z = x_1 + iy_1$ [61]. The table given in [61] does not give erfc ($x_1 + iy_1$) directly but an auxiliary function W_1 ($x_1 + iy_1$) that is defined as

$$\operatorname{erfc}(x_1 + iy_1) = W_1(-y_1 + ix_1)\, e^{-(x_1+iy_1)^2}$$

Some properties of $W_1(x_1 + iy_1)$ are

$$W_1(-x_1 + iy_1) = W_2(x_1 + iy_1)$$

$$W_1(x_1 - iy_1) = 2e^{-(x_1-iy_1)^2} - W_2(x_1 + iy_1)$$

where $W_2(x_1 + iy_1)$ is complex conjugate of $W_1(x_1 + iy_1)$.
Also v and Ψ are dummy variables and F_1, F_2, F_3, F_4 and F_5 are dummy functions.

Knowing the velocity field, we now study the changes in the skin-friction. It is given by:- $\tau^* = -\mu \left(\frac{\partial u^*}{\partial y^*}\right)_{y^*=0}$ (24)

The dimensionless expression for skin-friction evaluated from (19) is given by:

$$\tau = \frac{\tau^*}{\rho U_0^2} = -\left.\frac{du}{dy}\right|_{y=0} \tag{25}$$

$$= \frac{1}{\sqrt{\pi t}} + \frac{e^{i\omega t}}{2}\left[(1+i)\sqrt{\frac{\omega}{2}}\operatorname{erf}\left((1+i)\sqrt{\frac{\omega t}{2}}\right)\right] + \frac{e^{-i\omega t}}{2}\left[(1-i)\sqrt{\frac{\omega}{2}}\operatorname{erf}\left((1-i)\sqrt{\frac{\omega t}{2}}\right)\right]$$

$$+ \frac{a}{c}\left[1 - e^{c^2 t}\left(1+\operatorname{erf}(c\sqrt{t})\right)\right]\left(\sqrt{Pr_{eff}} - 1\right) + 2\sqrt{\frac{Pr_{eff}\, t}{\pi}} - 2a\sqrt{\frac{t}{\pi}} - 2b\sqrt{\frac{t}{\pi}}(Sc - 1) \tag{26}$$

Another phenomenon in this study is to understand the effects of t and Pr on Nusselt number. In non-dimensional form, the rate of heat transfer is given by:-

$$Nu = -\frac{\upsilon}{U_0\left(T^* - T_\infty^*\right)}\left.\frac{\partial T^*}{\partial y^*}\right|_{y^*=0} = \frac{1}{\theta(0)} + 1$$

$$= c\sqrt{Pr_{eff}}\left(1 + \frac{1}{e^{c^2 t}\left[1+\operatorname{erf}(c\sqrt{t})\right] - 1}\right) \tag{27}$$

The dimensionless expression of Sherwood number is given by:

$$Sh = -\left.\frac{\partial C}{\partial y}\right|_{y=0} = \sqrt{\frac{Sc}{\pi t}} \tag{28}$$

RESULTS AND DISCUSSION

In order to discuss the effect of various physical parameters on the velocity field, thermal boundary layer, concentration boundary layer, skin-friction, Nusselt number and Sherwood number the numerical computation of the analytical solutions, obtained in the preceding section, have been carried out and shown graphically. The regime is controlled by seven thermo-physical parameters which are radiation parameter (R), Prandtl number (Pr), Grashof number (Gr), modified Grashof number (Gm), Schmidt number (Sc), Newtonian heating parameter (γ), phase angle (ωt) and single geometric parameter which is angle of inclination (α) and time (t).

In figure 1 the evolution of dimensionless temperature profiles θ (y, t) inside the boundary layer, against span wise coordinate y for different values of Boltzmann-Rosseland radiation parameter R is shown. Again Pr = 0.71 i.e. Pr < 1, so that heat diffuses faster than momentum in the regime. $R = \frac{16\sigma T_\infty^{*3}}{3k k^*}$ and as discussed earlier this embodies

the relative contribution of heat transfer by thermal radiation to thermal conduction. R corresponds to an increase in the relative contribution of thermal radiation heat transfer to thermal conduction heat transfer. As for R<<1, thermal conduction heat transfer will dominate and vice versa for R > 1. Larger values of R therefore physically correspond to stronger thermal radiation flux and in accordance with this, the maximum temperatures are observed for R = 3. Rosseland's radiation diffusion model effectively enhances the thermal diffusivity, as described by Siegel and Howell. From this figure it is depicted that an increase in radiation parameter leads to an increase in the temperature in the boundary layer region which implies that radiation tends to enhance fluid temperature.

Figure 1: Temperature profiles for different values of radiation parameter R when t = 0.2, Pr = 0.71 and ϒ = 1.

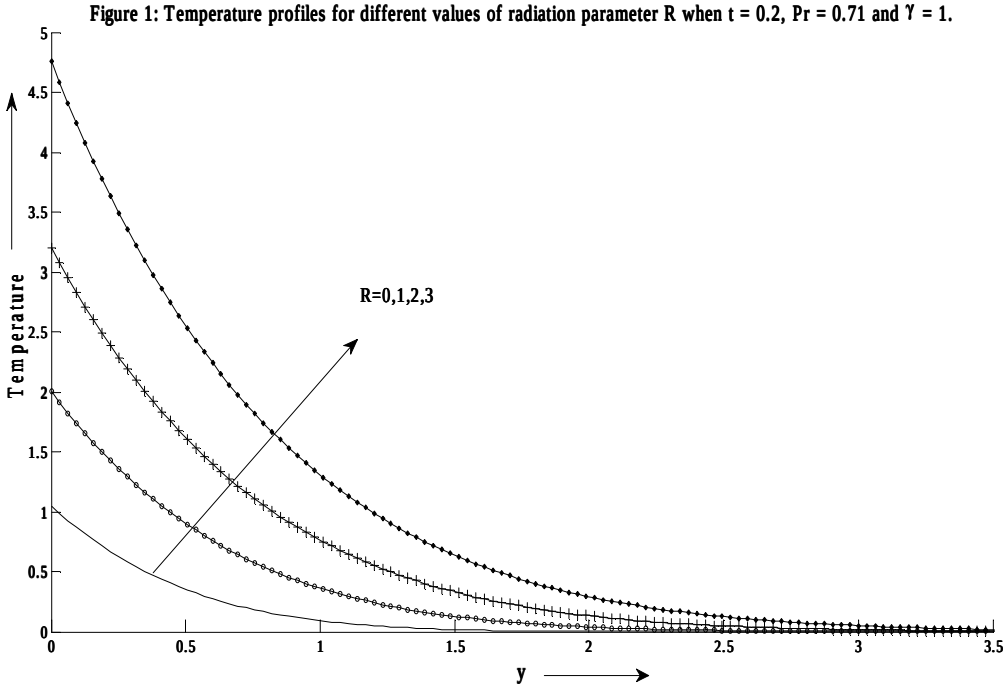

Figure 2 exhibits the influence of dimensionless time t on the thermal boundary layer. It is observed that there is an enhancement in fluid temperature as time progresses.

Figure 3 illustrates the influence of Prandtl number Pr on fluid temperature taking Pr = 0.71, 1.0, 7.0 and 100 which physically corresponds to air, electrolytic solution, water and engine oil respectively at 20^0C temperature and 1 atmospheric pressure. It is inferred that the thickness of thermal boundary layer is greatest for Pr = 0.71 (air), then for Pr = 1.0 (electrolytic solution) and then for Pr = 7.0 (water) and finally lowest for Pr = 100 (engine oil) ie. an increase in the Prandtl number results in a decrease of temperature. Pr signifies the relative effects of viscosity to thermal conductivity. The reason is that smaller values of Prandtl number are equivalent to increasing thermal conductivity and therefore heat is able to diffuse away from the heated surface more rapidly than for higher values of Prandtl number.

From figure 4 it is reported that an increase in the Newtonian heating parameter γ the thermal boundary layer thickness also increases and as a result the surface temperature of the plate increases. From figures 1 to 4 it is found that the maximum of the temperature occur in the vicinity of the plate and asymptotically approaches to zero in the free stream region.

In Figures 5 and 6 the concentration profiles are shown for different values of the Schmidt number Sc and time t respectively. Different values of Schmidt number Sc = 0.22, 0.3, 0.6, 0.78, 0.94 and 2.62 are chosen, they physically correspond to Hydrogen, Helium, water vapour, Ammonia, Carbon dioxide and Propyl Benzene respectively at 25^0C temperature and 1 atmospheric pressure. The profiles have a common feature that the concentration decreases exponentially from the surface to zero value far away in the free stream. A comparison of curves in the figures show

that the velocity decreases with increasing Schmidt number while the concentration boundary layer enhances for increasing times. This is consistent with the fact that the increase of Sc means decrease of molecular diffusivity that result in decrease of concentration boundary layer. Hence, the concentration of species is higher for small values of Sc and lower for large values of Sc.

Figure 2: Temperature profiles for different values of time t when R = 1,Pr = 0.71 and ϒ= 1.

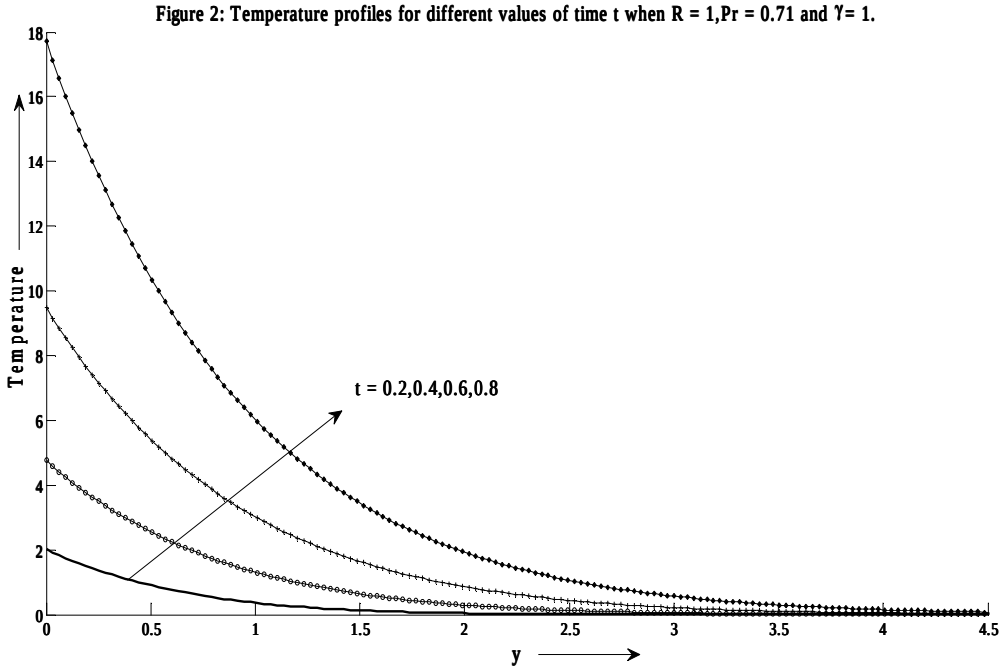

Figure 3: Temperature profiles for different values of Prandtl number Pr when R = 5, t = 0.2 and γ = 0.1

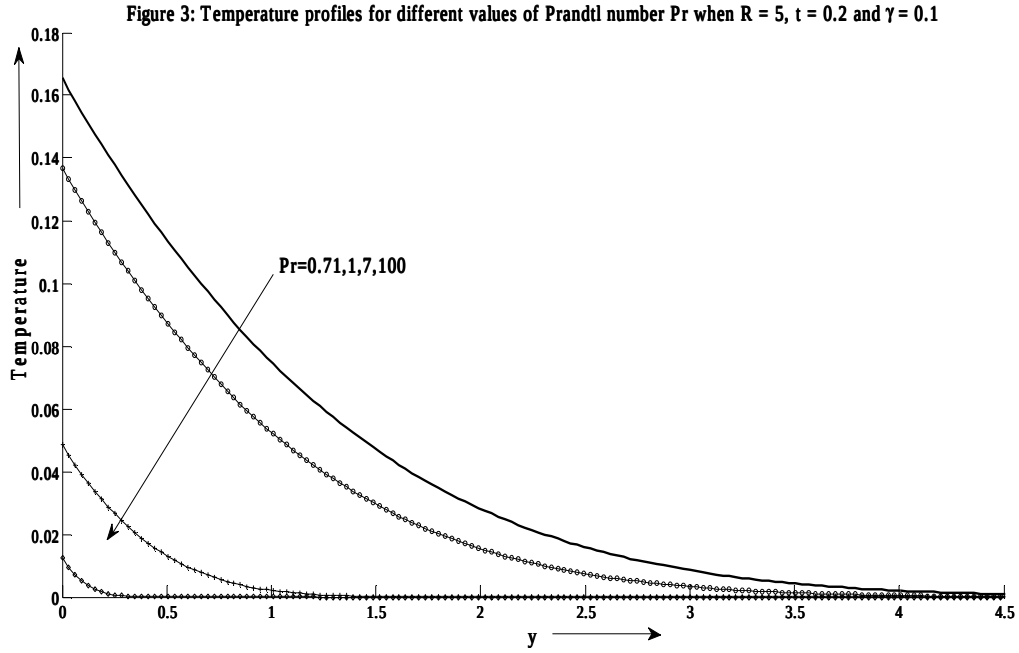

Figure 4: Temperature profiles for different values of Newtonian heating parameter γ when R = 1,Pr = 0.71 and t = 0.2.

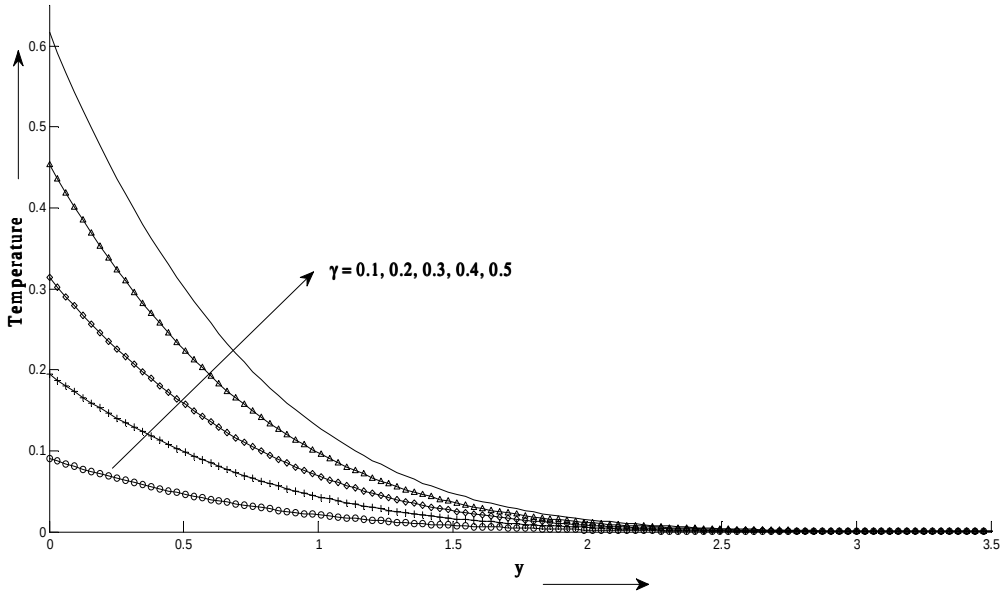

Figure 5: Concentration profiles for different values of Schmidt number Sc when t = 0.9.

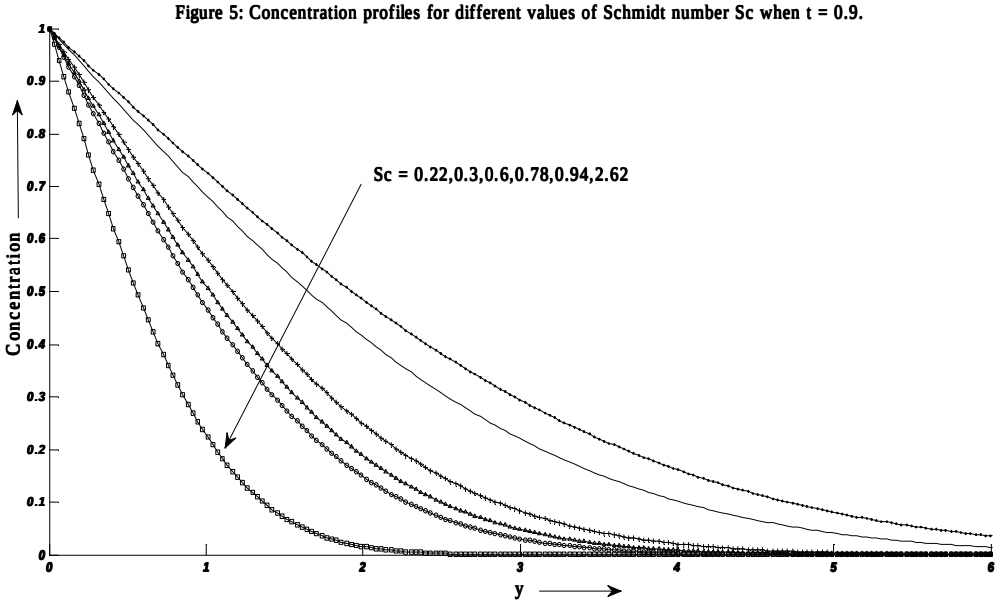

The velocity profiles u(y, t) in case of radiation and pure convection are shown in Figure 7. It is revealed from this figure that the radiation parameter R has an accelerating influence on fluid flow. Physically, it is due to the fact that an increase in the radiation parameter R for fixed values of other parameters decreases the rate of radiative heat transfer to the fluid, and consequently, the fluid velocity increases.

Figure 8 illustrates the influence of Prandtl number Pr on the flow field. It is evident from the figure that the fluid velocity overshoots the plate velocity in the regions close to the boundary. This overshooting is more pronounced for low Prandtl number fluids than for higher Prandtl number fluids. Also the thickness of momentum boundary layer is more for fluid with low Prandtl number. The reason underlying this behavior arises from the fact that the increase in the Prandtl number is due to the increase in the viscosity of the fluid, which makes the fluid thick and hence the fluid moves slowly. For Pr =1, the momentum and thermal boundary layers will have same thickness.

Figure 6: Concentration profiles for different values of time t Sc when Sc = 0.6.

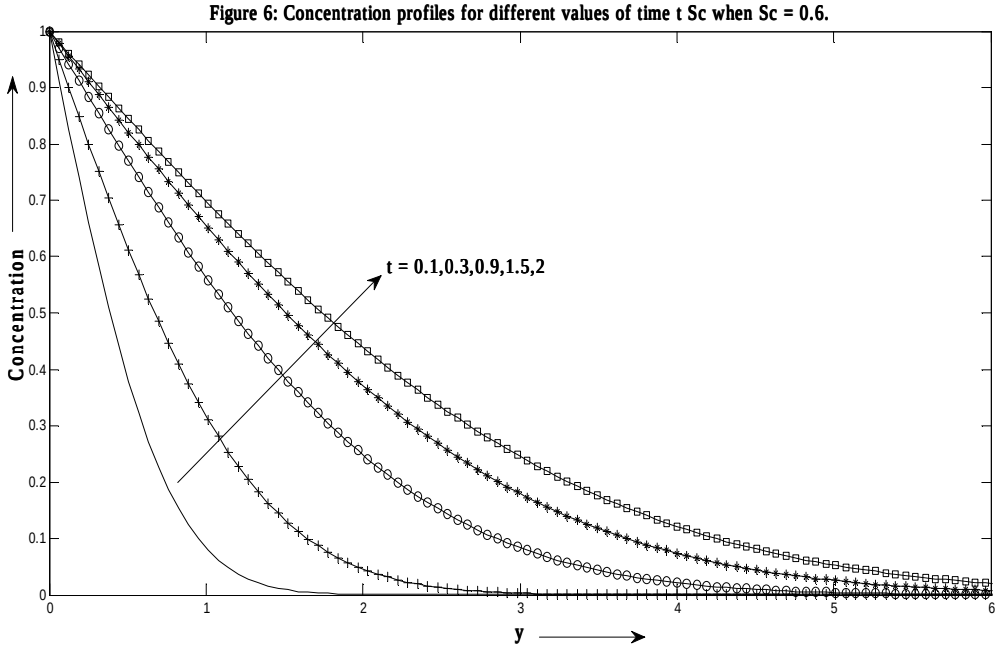

Figure 7: Velocity profiles for different values of radiation parameter R when Pr = 0.71,Sc = 0.3,Gr = 1,Gm = 3,t = 0.9, γ = 1,α = π/3,ωT=π/4

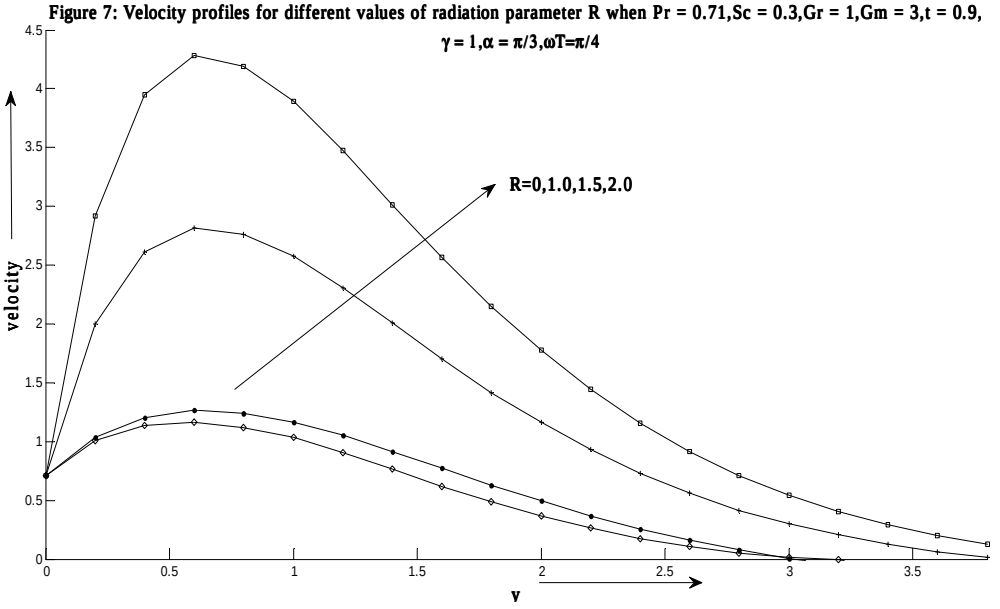

The effects of Grashof number Gr and modified Grashof number Gm on velocity are shown in figures 9 and 10. It is observed that the velocity increases with increasing values of Gr and Gm. Physically, this is possible because as the Grashof number and modified Grashof number increases, the contribution from the thermal and mass buoyancy near the plate becomes significant and hence a rise in the velocity near the plate is observed. This gives rise to an increase in the induced flow. For higher values of Gr, the fluid velocity overshoots the plate velocity in the regions close to the boundary.

Figure 11 displays the effects of Schmidt number Sc on the velocity field. It is inferred that the velocity decreases with increasing Schmidt number. An increasing Schmidt number implies that viscous forces dominate over the diffusion effects. Schmidt number in free convection flow regimes represents the relative effectiveness of

momentum and mass transport by diffusion in the velocity (momentum) and concentration (species) boundary layers. Smaller Sc values correspond to lower molecular weight species diffusing in air (eg. Hydrogen (Sc = 0.16), Helium (Sc = 0.3), water vapour (Sc = 0. 6), oxygen (Sc = 0.66), ammonia (Sc = 0.78), carbon dioxide (Sc = 0.96)) and higher values to denser hydrocarbons diffusing in air (e.g. Propyl benzene in air (Sc = 2.62). Effectively therefore an increase in Sc will counteract momentum diffusion since viscosity effects will increase and molecular diffusivity will be reduced. The flow will therefore be decelerated with a rise in Sc as testified by figure 11. It is also important to note that for Sc ~ 1, the velocity and concentration boundary layers will have the same thickness. For Sc < 1 species diffusion rate greatly exceeds the momentum diffusion rate and vice versa for Sc > 1.

Figure 8: Velocity profiles for different values of Prandtl numberPr when R = 2,Sc = 0.3,Gr = 1,Gm = 3,t = 0.9, γ = 1,α = π/3,ωT=π/4

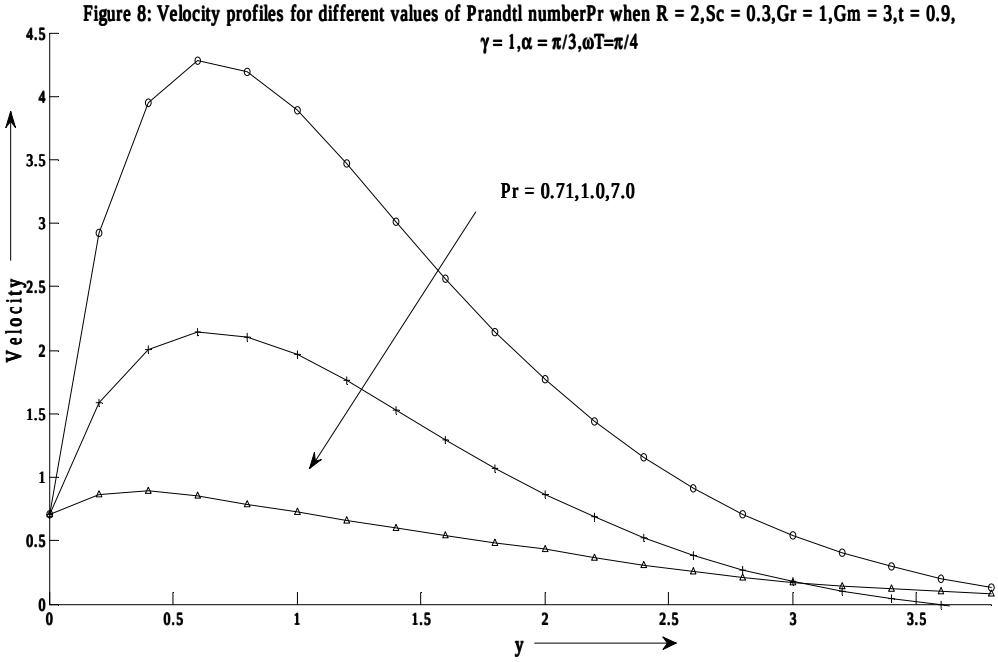

Figure 9: Velocity profiles for different values of Grashoff number Gr when R = 2,Sc = 0.3,Pr =0.71,Gm = 3,t = 0.9, γ = 1,α = π/3,ωT=π/4

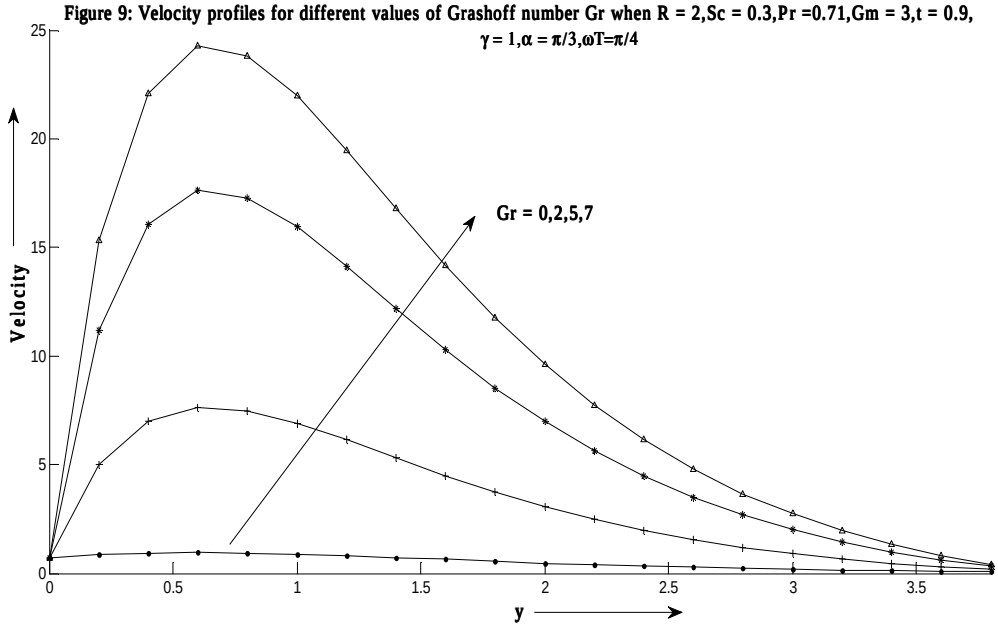

Figure 10: Velocity profiles for different values of Modified Grashoff number Gm when R = 2,Sc = 0.3,Pr =0.71,Gr = 1,t = 0.9, γ = 1,α = π/3,ωT=π/4

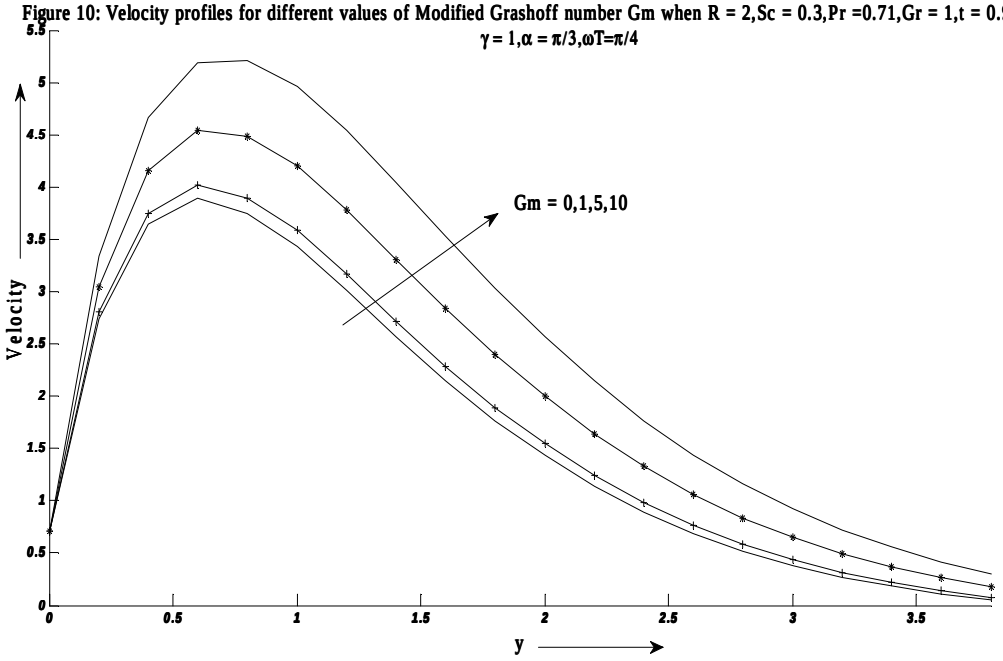

Figure 11:Velocity profiles for different values of Schmidt number Sc when R=0.1,Pr=0.71,Gr=10,Gm=20, t=0.9 γ = 1,α = π/3,ωT=π/4

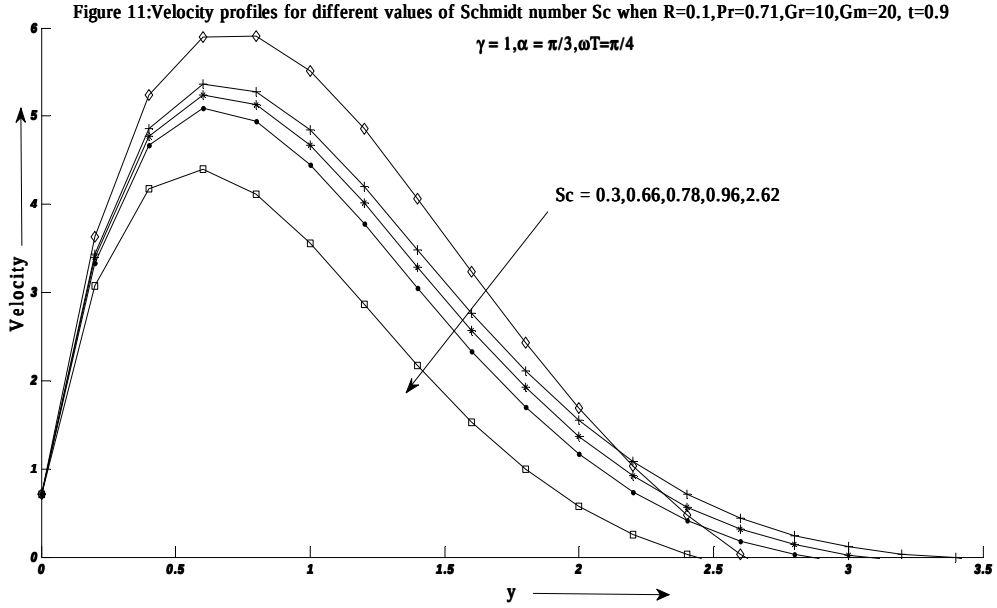

Figure 12 displays the effect of Newtonian heating parameter γ on the dimensionless velocity. It is found that as the Newtonian heating parameter increases the density of the fluid decreases, and the momentum boundary layer thickness increases and as a result the velocity increases within the boundary layer.

Representative velocity profiles for five typical angles of inclination (α = 0, π/6, π/4, π/3, π/2) are presented in figure 13. It is revealed from this figure that on increasing the angle of inclination, the velocity decreases. The fact is that as the angle of inclination increases the effect of the buoyancy force due to thermal and mass diffusion decrease by a factor of cos α. Consequently the driving force to the fluid decreases and as a result velocity profiles decrease. From this figure it is also noticeable that the effect of buoyancy force (which is maximum for α = 0) overshoots the main stream velocity significantly.

Figure 12:Velocity profiles for different values of Newton Heating parameterγ when R=2,Pr=0.71,Sc=0.3,Gr=2,Gm=2, t=0.9

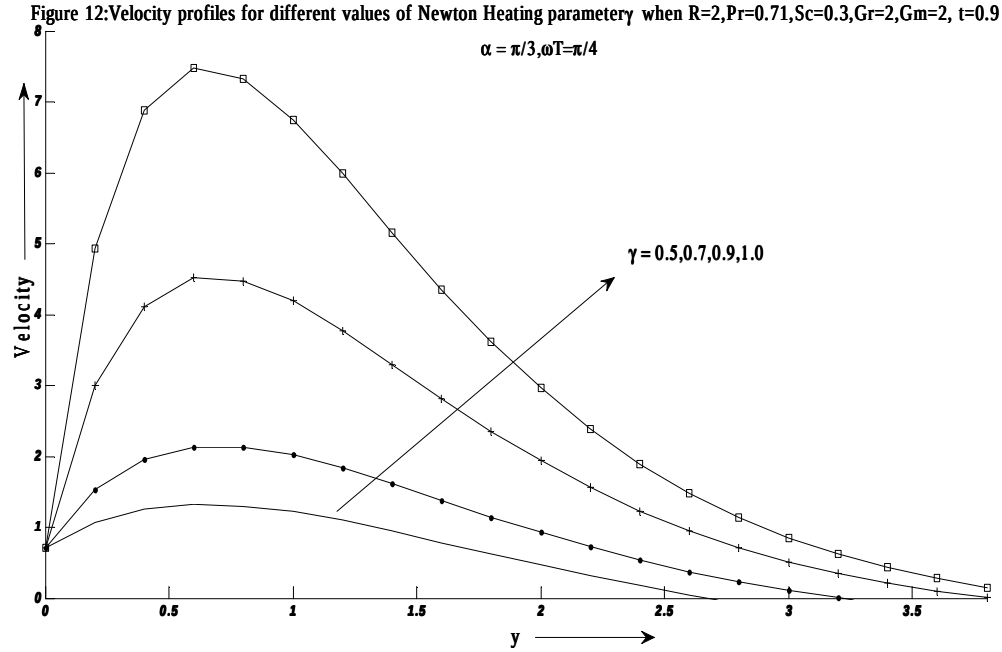

Figure 13:Velocity profiles for different values of angle of inclination when R=2,Pr=0.71,Sc=0.94,Gr=2,Gm=2, t=0.9

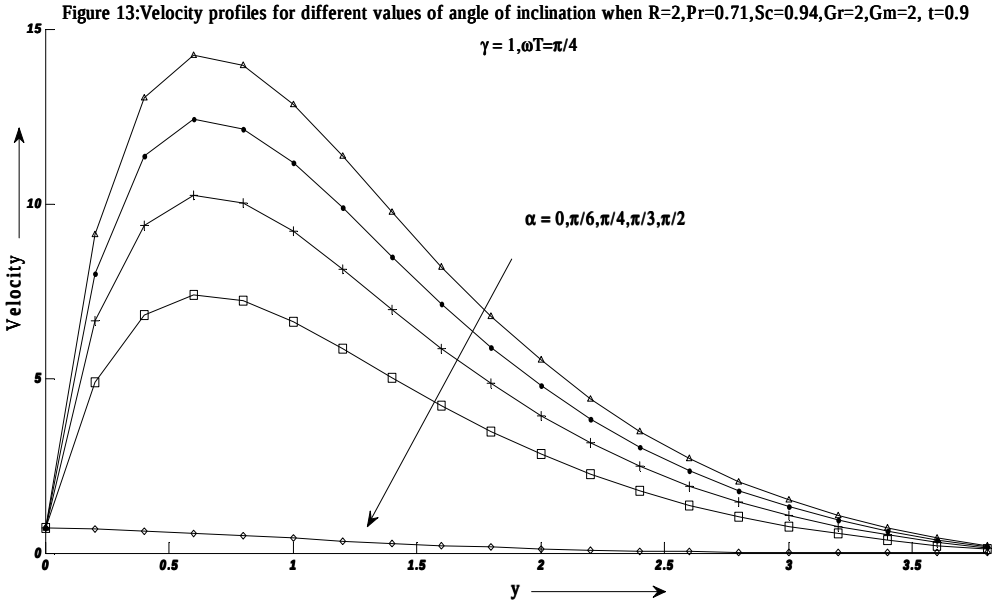

The variation of fluid velocity u(y, t) due to the oscillation of the plate is depicted in figure 14 taking fluids as water (Pr = 7.0) and air (Pr = 0.71). The boundary condition for y→ ∞ is replaced by identical ones at y_{max} where the velocity profiles decay to the relevant boundary condition. We choose y_{max} = 4.0. It is noticed that on increasing phase angle ωt from 0 to π/2 the plate velocity decreases. A comparative study of data presented in figure 14 show that the thickness of momentum boundary layer is greater for Pr = 0.71 as compared to Pr = 7.0. The inverse variation of temperature with the Prandtl number is also observed for velocity. The phase angle ωt = 0 corresponds to no oscillation of the plate, then the fluid approaches to its maximum velocity of magnitude 1 whereas for the phase angle ωt = π/2, the velocity gains its minimum value of magnitude 0. The oscillations near the plate are of great significance; however, these oscillations reduce for large values of the independent variable y and approach to zero as y tends to infinity.

Figure 14:Velocity profiles for different values of phase angle when R=0.2,Sc=0.22,Gr=1,Gm=5, t=0.9, γ = 1,α=π/3

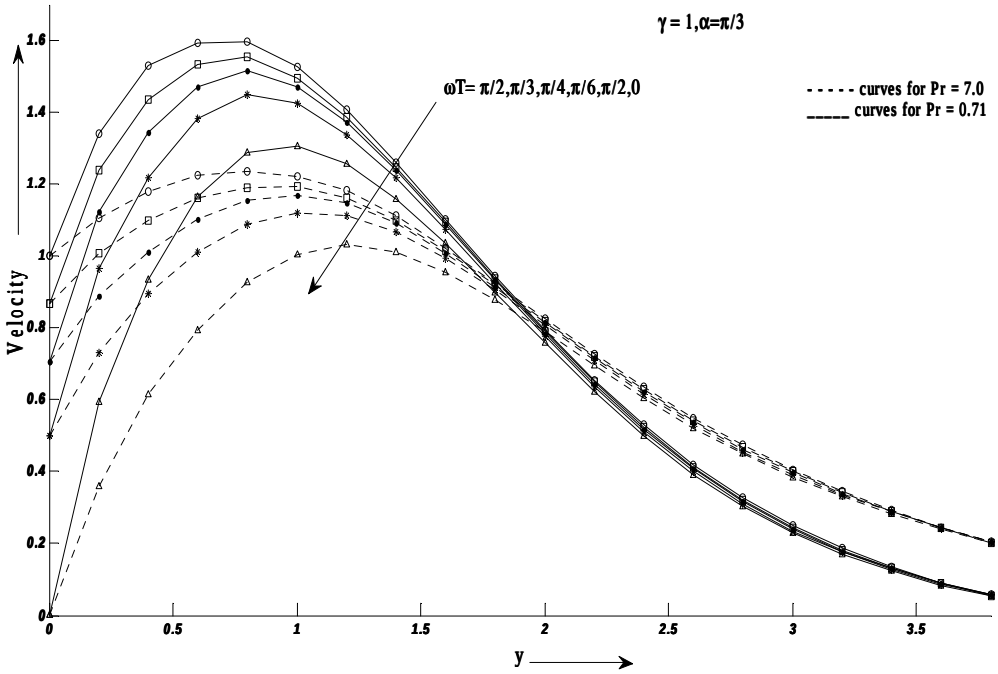

Figure 15:Velocity profiles for different values of time t when R=0.2,Sc=0.3,Gr=1,Gm=5,Pr=0.71, γ = 1,α=π/3

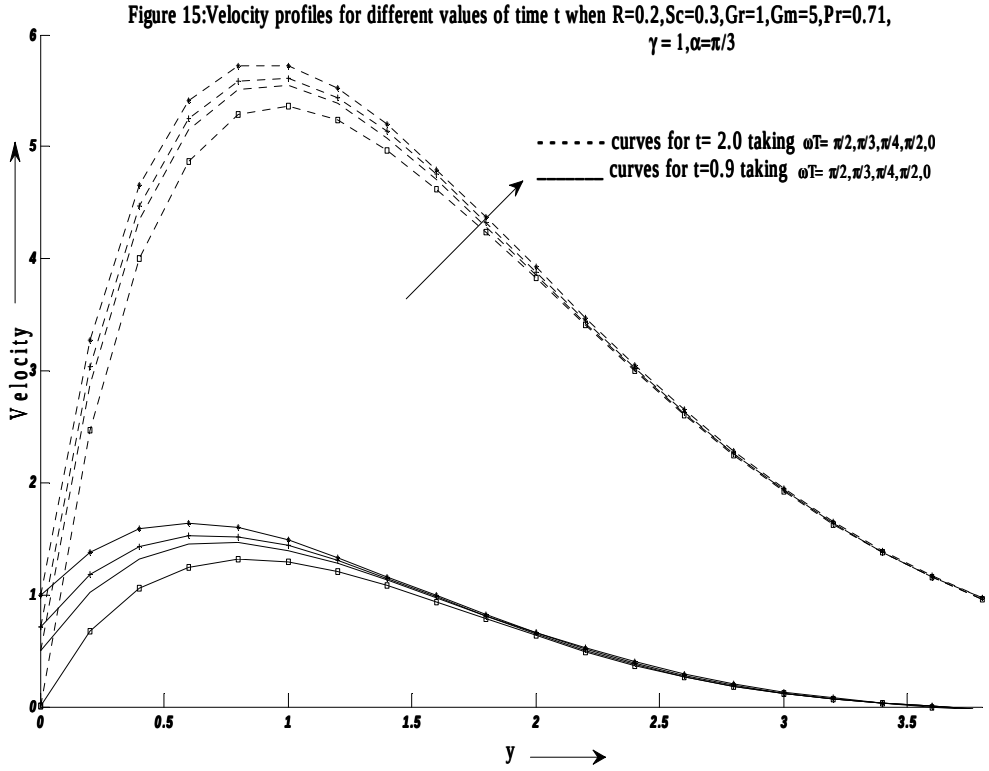

Fig.16(a):Variation of Skin friction for various values of Schimdt number(Sc), Newtonian heating parameter(γ),angle of inclination(α) taking Pr = 0.71, R=0.2, Gr =3, Gm = 5.

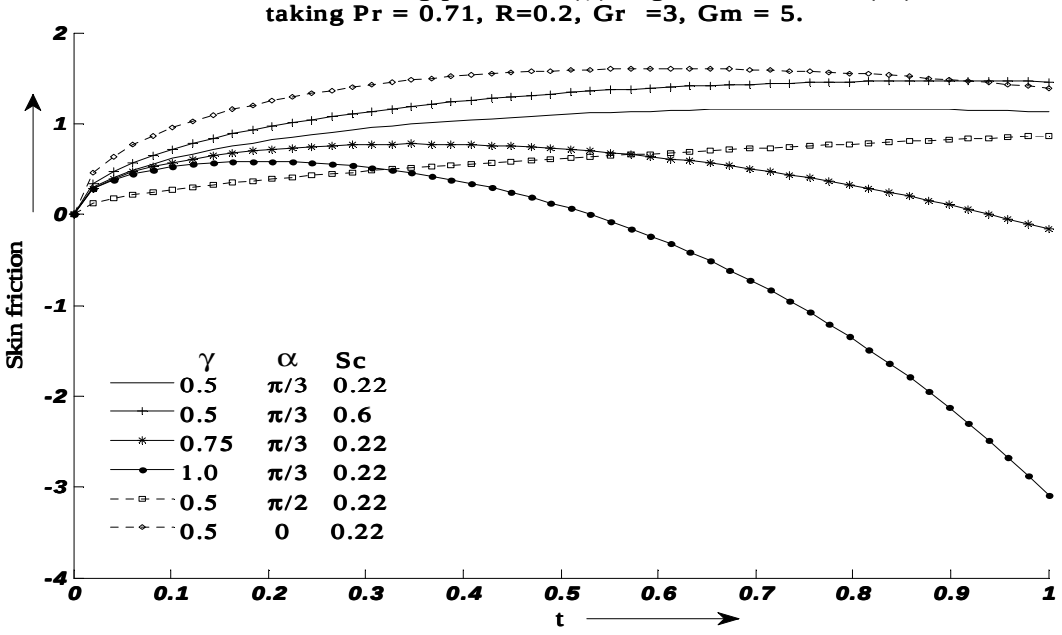

Fig.16(b):Variation of Skin friction for various values of Grashof number(Gr),modifiedGrashof number(Gm), Radiation parameter(R),Prandtl number(Pr),taking Sc=0.22, γ = 0.5,α =π/3

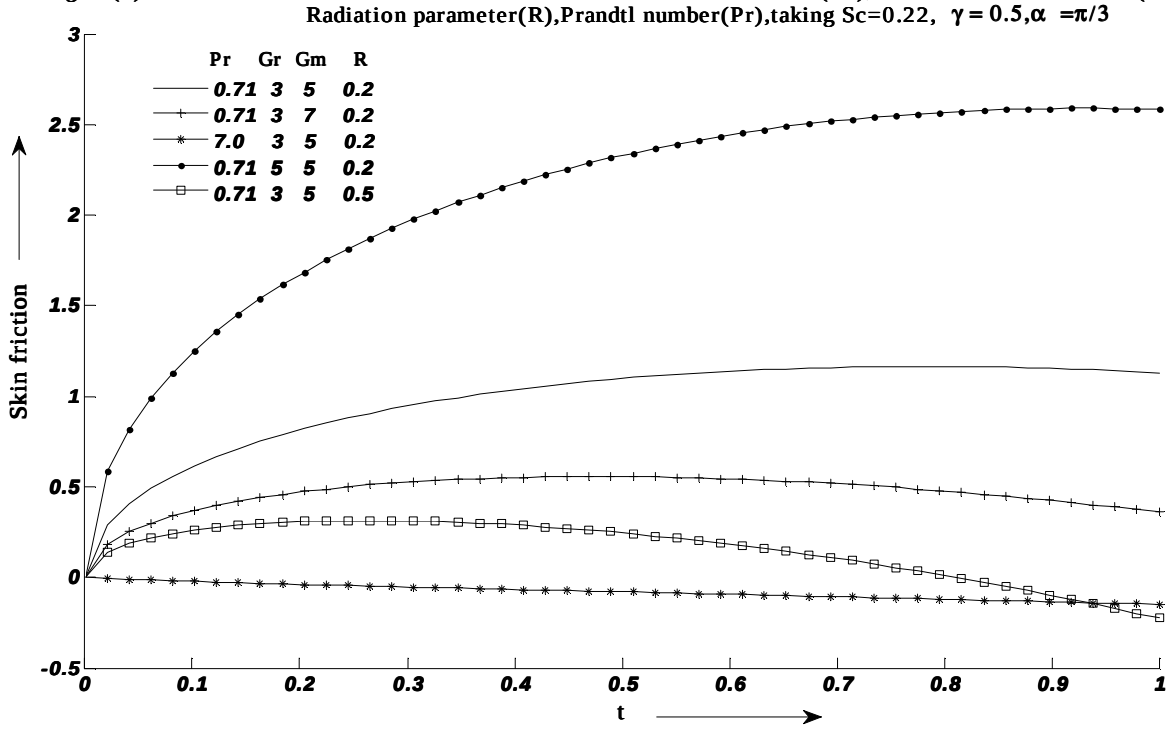

Figure 17: Variation of Nusselt number for different values of Prandtl number (Pr),radiation parameter (R), Newtonian heating Parameter (γ).

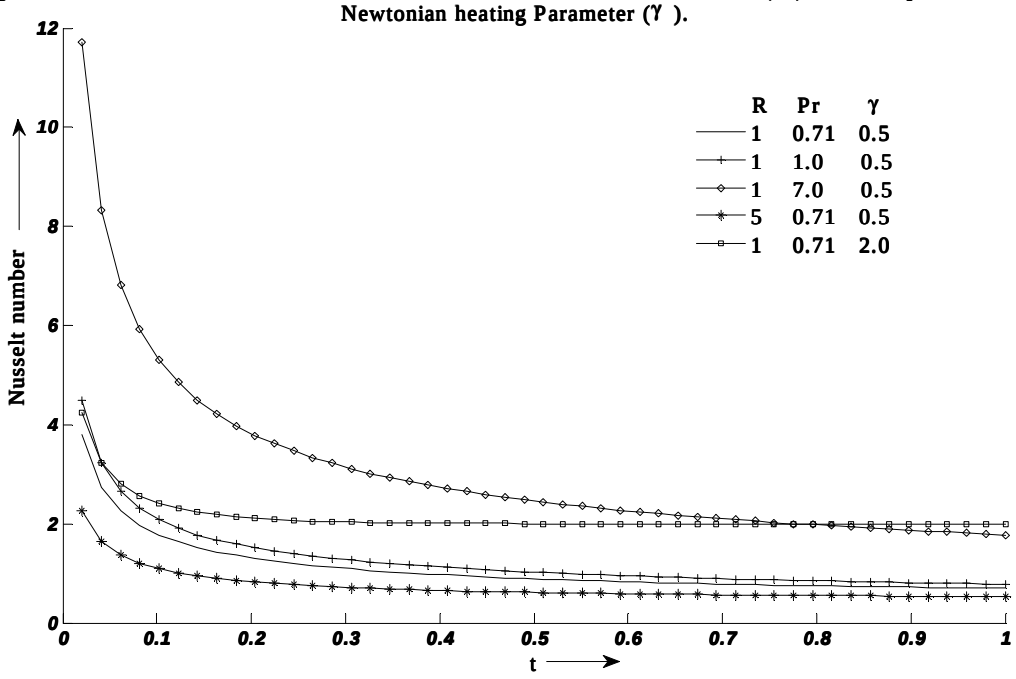

Figure 18: Sherwood number variation for different values of Schimdt number (Sc).

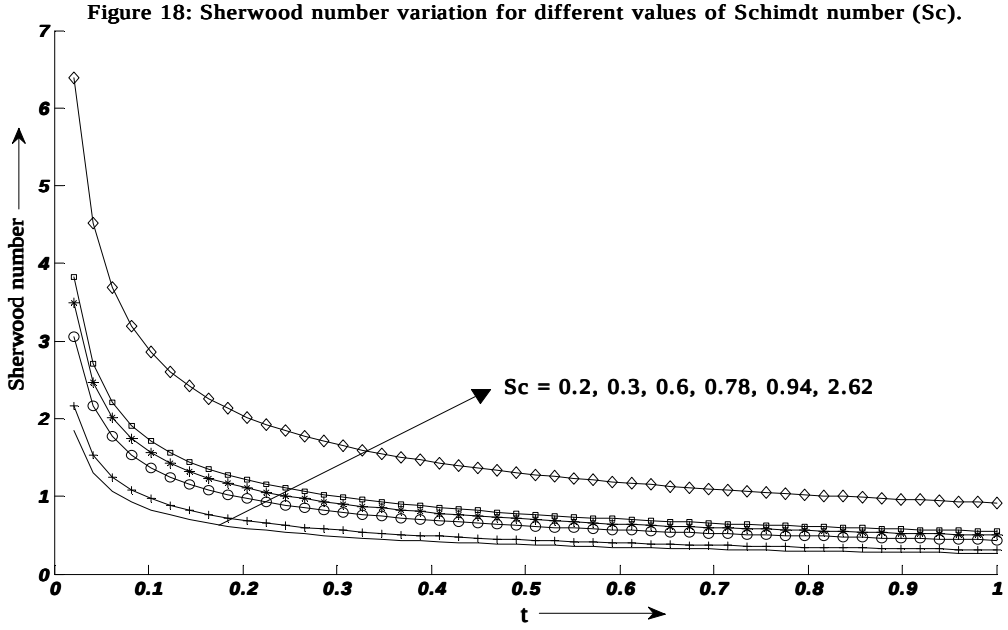

In order to highlight the effect of temporal variable t on the flow field figure 15 is presented herein taking different phase angles ωt is revealed that as the time progresses the thickness of momentum boundary layer increases because the contribution from the buoyancy force near the plate become significant and hence the velocity increases monotonically with the temporal variable t. From figures 7-15 we observe that the velocity becomes maximum in the vicinity of the plate and then decreases away from the plate and finally takes asymptotic values far away from the plate.

Figure 16(a) illustrates the combined effects of Schmidt number (Sc), angle of inclination (α) and Newtonian heating parameter (γ) on skin friction when plotted against time t taking ωt = π/2. It is found that an increase in the

angle of inclination would produce a decrease in the buoyancy force s and hence reduce the skin friction coefficient. For horizontal plate ($\alpha = \pi/2$) as expected the velocity is minimized since gravitational acceleration effects are negated. With a decrease in angle of inclination to $\pi/3$ and eventually to the minimum (vertical) orientation ($\alpha = 0$) the flow is strongly accelerated as gravitational acceleration effects are maximized. Similar effect is exhibited on increasing the Newtonian heating parameter i.e. skin friction reduces on increasing γ whereas on increasing Schimdt number it increases.

Figure 16(b) elucidates that with increasing radiation (R), Prandtl number (Pr) and modified Grashof number (Gm) frictional shear stress decreases while reverse happens for increasing Grashof number (Gr). It is investigated that skin friction falls with an increase in Pr, physically, this is true because an increase in the Prandtl number is due to increase in the viscosity of the fluid, which makes the fluid thick and hence a decrease in the velocity of the fluid. Therefore skin friction decreases with increasing Pr.

Figure 17 displays dimensionless rate of heat transfer Nusselt number (Nu) against time t. This figure shows that increasing Prandtl number and Newtonian heating parameter γ enhances the heat transfer coefficient. This may be explained by the fact that frictional forces become dominant with increasing values of Pr and yield greater heat transfer rate. Furthermore, as time advances, the value of Nu is decreasing and after some time it becomes constant. Nusselt number decreases on increasing radiation R which implies that radiation tends to reduce rate of heat transfer at the plate.

From figure 18, it is observed that the Sherwood number increases with increasing Sc, while reverse happens for increasing time t.

The present analytical (Laplace transform) solutions provide other researchers with solid benchmarks for numerical comparisons. The authors have used this method in other articles where they have bench marked approximate methods such as numerical, asymptotic or experimental methods against analytical (Laplace transform) solutions. Further, all these graphical results discussed above are in good agreement with the imposed boundary conditions given by (12). Hence, this ensures the accuracy of our results.

Nomenclature

C_p	Specific heat at constant pressure
C^*	Species concentration in the fluid
C^*_w	Species concentration near the plate
C^*_∞	Species concentration in the fluid far away from the plate
C	Dimensionless concentration
D	Mass diffusivity
g	Magnitude of the acceleration due to gravity
h	Heat transfer coefficient
k	Thermal conductivity of the fluid
k^*	Mean absorption coefficient
Gr	Thermal Grashof number
Gm	Modified Grashof number
Pr	Prandtl number
q_r	Radiative heat flux in the y^* direction
R	Radiation parameter
Sc	Schmidt number
T^*	Temperature of the fluid
T^*_∞	Ambient temperature
t^*	Time
t	Non-dimensional time
u^*	Dimensional velocity along x^*-direction
u(y,t)	Dimensionless velocity
y^*	Cartesian coordinate normal to the plate

y Dimensionless coordinate axis normal to the plate

Greek symbols

α Angle of inclination of the plate
β Volumetric Coefficient of thermal expansion
β^* Volumetric Coefficient of mass expansion
ρ Density of the fluid
θ Dimensionless temperature
μ Coefficient of viscosity
ν Kinematic viscosity
σ Stefan-Boltzmann constant
τ^* Skin-friction
τ Dimensionless skin-friction
θ Dimensionless temperature
ω Frequency of oscillation
ωt Phase angle

CONCLUSION

An exact solution of the unsteady free convection boundary-layer flow of an incompressible fluid past an inclined oscillating plate with the flow generated by Newtonian heating in the presence of radiation was studied. The resulting coupled linear partial differential equations which describe the problem are non-dimensionalized and their solutions have been obtained in closed form with the help of Laplace-transform technique. The obtained solutions satisfy governing equations as well as the boundary conditions are discussed through graphs for different values of parameters entering into the problem. The following conclusions can be drawn from the results obtained:

1.The dimensionless temperature profiles increase with increase in radiation parameter, time and Newtonian heating parameter whereas reverse happen for increasing Prandtl number.

2.The dimensionless concentration profiles decrease with increase in Schimidt number while reverse happen for increasing time.

3.The dimensionless velocity profiles increase with increase in radiation parameter, Grashoff number, Modified Grashoff number, Newtonian heating parameter and time while the thichness of momentum boundary decrease with increase in Prandtl number, Schimdt number, angle of inclination of the plate and phase angle ωt of the oscillating plate.

4.Skin-friction profiles show an increase with increase in Schimdt number while the increase in angle of inclination of the plate and newtonian heating parameter the dimensionless skin friction profiles decrease.

5.Dimensionless rate of heat transfer which is Nusselt number increases as Prandtl number and Newtonian heating parameter enhances but contrary to this, as time and radiation parameter increases the rate of heat transfer decreases.

6.The Sherwood number increases with increasing Schimdt number, while reverse happens for increasing time t.

REFERENCES

[1] Soundalgekar V.M, *Journal of Heat Transfer, Transactions of the ASME*, **1977,** 99, 499-501.
[2] Singh A.K., Naveen Kumar, *Astrophysics and Space*, **1984,** 98, 245-258.
[3] Hossain M.A., Shayo L.K., *Astrophysics and Space*, **1986,** 125, 315-324.
[4] Das U.N., Deka R.K., Soundalgekar V.M., *Journal of Heat Transfer Transactions of the ASME*, **1999,**121, 1091-1094.
[5] Soundalgekar V.M., Deka R.K., Das U.N., *Indian Journal of Engineering and Materials Sciences***, 2003,** 10, 390-396.
[6] Stuart J.T.,*Recent Research on Unsteady Boundary Layers*, Lavel University Press, Quibec, **1972**
[7] Telionis D.P., *Unsteady Viscous Flows*, Springer-Verlag, New York, **1981**
[8]Pop I.,*Theory of Unsteady Boundary Layers*, Romanian Academy of Sciences, and Bucharest, **1983**
[9]Raptis A. ,Perdikis C., *Forschung im Ingeneiurwesen– Engineering Research*, **2002,** 67 (5), 206-208.
[10] Das U.N., Deka R.K., Soundalgekar V.M., *Journal of Heat Transfer*, **1999,**121, 1091-1094.

[11] Muthucumaraswamy R., *Far East Journal of Applied Mathematics*, **2004,** 14 (1), 99-109.
[12] Chandran Pallath, Sacheti N.C., Singh A.K, *Heat and Mass Transfer*, **2005,** 41(5), 459-464.
[13] Gebhart B., Pera L, *International Journal of Heat Mass Transfer*, **1971,** 14, 2025-2050.
[14] Soundalgekar V.M., *ASME Journal of Applied Mechanics*, **1979,** 46, 757-760.
[15] Soundalgekar V.M., Birajdar N.S., Darwheka V.K., *Astrophysics and Space Science*, **1984**, 100,159-164.
[16] Soundalgekar V.M., Pohanerkar S.G., Lahurikar R.M., *Forschung im Ingenieurwesen – Engineering Research*, **1992**, 58, 63-66.
[17] Das U.N., Deka R., Soundalgekar V.M., *Forschung im Ingenieurwesen – Engineering Research*, **1994**, 60, 284-287.
[18] Das U.N., Ray S.N., Soundalgekar V.M., *Heat and Mass Transfer*, **1996,** 31, 163-167.
[19] Jha B.K., Prasad R., Rai, S., *Astrophysics and Space Science*, **1991,** 181, 125-134.
[20] Muthucumaraswamy R. , Sathappan K. E., Natarajan R., *International Journal of Applied Mathematics and Mechanic.*, **2008,** 4, 19-25.
[21] Muthucumaraswamy R., Sathappan K. E., Natarajan R, *Theoretical and Applied Mechanics*, **2008,** 35 (4), 323-331.
[22] Narahari M., Beg O. A., Ghosh S. K,*World Journal of Mechanics*, **2011,**1,176-184.
[23]R. Saravana, S. Sreekanth, S. Sreenadh, R. Hemadri Reddy, *Advances in Applied Science Research*, **2011**, 2 (1), 221-229.
[24] Stokes G.G, *Transactions Cambridge Philosophical Society*, **1851,** IX, 8-106.
[25] Soundalgekar V.M, *Astrophysics and Space Science*, **1979**, 64, 165-171.
[26] Turbatu S., Bühler K., Zierep J., *Acta Mechanica*, **1998,** 129, 25-30.
[27] Revankar S.T., *Mechanics Research Communication*, **2000,** 27, 241-246.
[28] Gupta, A.S., Misra, J.C., Reza, M., Soundalgekar, V.M, Acta Mechanica, **2003,** 165,1-16.
[29] R. M. Lahurikar, V. M. Soundalgekar, S. G. Pohanerkar, N. S. Birajdar, *Heat and Mass Transfer*. **1995**, 30 (5), 309–312.
[30] Hossain M.A., Alim M.A., Rees D.A.S., *International Journal of Heat and Mass Transfer*, **1999,** 42,181-191.
[31] Raptis A., Perdiki, C, Applied *Mechanics and Engineering*, **1999**, 4(4), 817-821.
[32] Soundalgekar V.M., Das U.N. and Deka R.K., *Journal of Theoretical and Applied Fluid Mechanics*, **1996,** 1, 111-115.
[33] M. A. Hossain, H. S. Takhar, *Heat and Mass Transfer*, **1996,** 31(4), 243-248.
[34] Makinde O.D., *International Communication in Heat and Mass Transfer*, **2005,** 32(10), 1411-1419.
[35] Muthucumaraswamy R., Chandrakala P., *Forschung im Ingenieurwese– Engineering Research*, **2005,** 69(4), 205-208.
[36] Muthucumaraswamy R. , *Theoretical and Applied Mechanics*, **2010,** 37(1), 1-15.
[37] Deka R. K., Das S. K, *Engineering*, **2011**, 3, 1197-1206.
[38] Jana R. N. , Ghosh S.K, *World Journal of Mechanics*, **2011,** 1, 64-69.
[39] Sib Sankar Manna, Sanatan Das and Rabindra Nath Jana, *Advances in Applied Science Research***, 2012,** 3 (6), 3722-3736.
[40]K. Raveendra Babu, A.G. Vijaya Kumar, S.V.K. Varma, *Advances in Applied Science Research*, **2012**, 3 (4), 2446-2462
[41]B. Seshaiah, A. G. Vijaya kumar and S. V. K. Varma, *Advances in Applied Science Research*, **2012,** 3 (5), 3273-3284
[42] Jayaraj S., Heat *and Mass Transfer*, **1995,** 30(3), 167-173.
[43] Doroodchi E., Galvin K.P., Fletcher, D.F., Powder *Technology*, **2005,** 156, 1-7.
[44]Bég O. Anwar, Bég TA, Bakier AY, Prasad V.R., *International Journal of Applied Mathematics and Mechanics*, **2009,** 5, 39-57.
[45]Ghosh S. K., Rwat S., Beg O. A., Beg T.A., *International Journal of Applied Mathematics and Mechanics*, **2010,** 6(13), 41-57.
[42] Barik R.N. *Asian Journal of Current Engineering and Maths*, **2013,** 2 106-114.
[47] Reddy S., Reddy G.V.R. and Reddy K.J., *Asian Journal of Current Engineering and Maths*, **2012,** 1, 115-119.
[48] Merkin, J.H, International *Journal of* Heat *Fluid Flow*, **1994,** 15, 392-398.
[49] Lesnic D., Ingham D.B., Pop, I., *International Journal of* Heat *Mass Transfer*, **1999,** 42, 2621-2627.
[50] *Ibid*, *Journal of Porous Media*, **2000,** 3, 227-235.
[51] Lesnic D., Ingham D.B., Pop I., Storr, C., *Heat and Mass Transfer*, **2003,** 40 (4), 665-672.
[52] Chaudhary R.C., Jain Preeti, Romanian *Journal of Physics*, **2006,** 51, 911-925.
[53] Chaudhary R.C., Jain Preeti, *Journal of Engineering Physics and Thermophysics*, **2007,** 80, 954-960.

[54] Narahari M., Nayan M.Y, *Turkish Journal of Engineering and Environmental Sciences*, **2011,** 35,187-198.
[55] Raju K.V.S., Reddy T.S., Raju M.C., Venkataramana, *International Journal of Mathematics and Computer Application Research*, **2013,** 3(2), 215-226.
[56] Narahari M., Ishak A, *Journal of Applied Sciences*, **2011,** 11(7), 1096-1104.
[57] Mebine P., Adigio E.M., *Turkish Journal of Physics*, **2009,** 33, 109-119.
[58] R. Siegel, J. R. Howell, *Thermal Radiation Heat Transfer*, Taylor & Francis, New York, NY, USA, **2002,**4th edition.
[59] Salleh M. Z., Nazar R.,Pop I., *Journal of the Taiwan Institute of Chemical Engineers*, **2010,** 41(6), 651–655.
[60] Kasim A. R. M., Mohammad N. F., Aurangzaib, Sharidan S., *World Academy of Science, Engineering and Technology*, **2012,** 64, 628–633.
[61]Abramowitz B.M., Stegun I.A., *Handbook of Mathematical Functions*, Dover Publication, Inc., New York, **1972**